Geochemistry Geophysics Geosystems G3
AN ELECTRONIC JOURNAL OF THE EARTH SCIENCES
Published by AGU and the Geochemical Society

Article
Volume 9, Number 2
8 February 2008
Q02S03, doi:10.1029/2007GC001826
ISSN: 1525-2027

Pacific offshore record of plinian arc volcanism in Central America: 3. Application to forearc geology

S. Kutterolf
SFB574 at Kiel University/IFM-GEOMAR, Wischhofstrasse 1-3, D-24148 Kiel, Germany (skutterolf@ifm-geomar.de)

A. Freundt
SFB574 at Kiel University/IFM-GEOMAR, Wischhofstrasse 1-3, D-24148 Kiel, Germany

IFM-GEOMAR, Wischhofstrasse 1-3, D-24148 Kiel, Germany

U. Schacht
SFB574 at Kiel University/IFM-GEOMAR, Wischhofstrasse 1-3, D-24148 Kiel, Germany

CO2CRC, Australian School of Petroleum, University of Adelaide, Adelaide, South Australia 5005, Australia

D. Bürk and R. Harders
SFB574 at Kiel University/IFM-GEOMAR, Wischhofstrasse 1-3, D-24148 Kiel, Germany

T. Mörz
MARUM, Leobener Strasse, D-28359 Bremen, Germany

W. Peréz
SFB574 at Kiel University/IFM-GEOMAR, Wischhofstrasse 1-3, D-24148 Kiel, Germany

[1] Sediment gravity cores collected on the Pacific slope and incoming plate offshore Central America reach up to 400 ka back in time and contain numerous ash layers from plinian eruptions at the Central American Volcanic Arc. The compositionally distinct widespread ash layers form a framework of marker horizons that allow us to stratigraphically correlate the sediment successions along and across the Middle America Trench. Moreover, ash layers correlated with 26 known eruptions on land provide absolute time lines through these successions. Having demonstrated the correlations in part 1, we here investigate implications for submarine sedimentary processes. Average accumulation rates of pelagic sediment packages constrained by bracketing tephras of known age range from ~1–6 cm/ka on the incoming plate to 30–40 cm/ka on the continental slope. There are time intervals in which the apparent pelagic sedimentation rates significantly vary laterally both on the forearc and on the incoming plate where steady conditions are usually expected. A period of unsteadiness at 17–25 ka on the forearc coincides with a period of intense erosion on land probably triggered by tectonic processes. Unsteady conditions on the incoming plate are attributed to bend faulting across the outer rise triggering erosion and resedimentation. Extremely low apparent sedimentation rates at time intervals >50–80 ka suggest stronger tectonic activity than during younger times and indicate bend faulting is unsteady on a longer timescale. Submarine landslides are often associated with ash layers forming structurally weak zones used for detachment. Ash beds constrain ages of >60 ka, ~19 ka, and <6 ka for three landslides offshore Nicaragua. Phases of intense fluid venting at mud mounds produce typical sediments around the mound that become covered by normal

pelagic sediment during phases of weak or no activity. Using intercalated ash layers, we determine for the first time the durations (several hundred to 9000 years) of highly active periods in the multistage growth history of mud mounds offshore Central America, which is essential to understand general mud-mound dynamics.

Components: 7470 words, 7 figures, 1 table.

Keywords: marine tephrostratigraphy; plinian volcanism; forearc geology; submarine slides; mound structures; Central America.

Index Terms: 8455 Volcanology: Tephrochronology (1145); 8428 Volcanology: Explosive volcanism; 4219 Oceanography: General: Continental shelf and slope processes (3002).

Received 13 September 2007; **Revised** 15 October 2007; **Accepted** 23 October 2007; **Published** 8 February 2008.

Kutterolf, S., A. Freundt, U. Schacht, D. Bürk, R. Harders, T. Mörz, and W. Peréz (2008), Pacific offshore record of plinian arc volcanism in Central America: 3. Application to forearc geology, *Geochem. Geophys. Geosyst.*, *9*, Q02S03, doi:10.1029/2007GC001826.

Theme: Central American Subduction System
Guest Editors: G. Alvarado, K. Hoernle, and E. Silver

1. Introduction

[2] Ash from numerous plinian, phreatoplinian and ignimbrite-forming eruptions from volcanic complexes along the Central American Volcanic Arc (CAVA) was dispersed far westward across the Pacific to form widespread ash layers extending >400 km from vent across 10^6 km^2 [*Kutterolf et al.*, 2007b, 2008a]. The 56 gravity cores of up to 11 m length we have drilled along the Middle America Trench on both the forearc and the incoming plate (Figure 1) contain the record of tephras and intercalated sediments reaching back to 400 ka. Distinct compositional characteristics of the ash layers allow their correlation between cores and with tephras exposed on land as shown in part 1 [*Kutterolf et al.*, 2008a], where we have identified the distal ashes of 26 large eruptions at the CAVA and constrained the ages of 10 previously undated eruptions from the marine record. In part 2 we have used these correlations to determine the distribution characteristics of the tephras and their erupted magma masses which we combined with published data to derive long-term magma discharge rates for the individual volcanic systems as well as the whole CAVA [*Kutterolf et al.*, 2008b]. Here we use the tephra record to constrain geological processes on the Pacific seafloor.

[3] The Central American Pacific forearc is characterized by the tectonics of subduction erosion, by numerous sites of localized fluid venting (Figure 1), and by submarine landslides triggered by gas hydrate dissolution or seamount subduction. During recent years these structures have been imaged in great detail by high resolution bathymetry and seismic profiling accompanied by geochemical analyses of vent fluids and biogeochemical studies of vent fauna. However, these methods do not determine the ages of such structures and their formation events. Ash layer provide a tool to determine sedimentation rates and formation ages, which we here use to date failures of the continental slope and to determine the "life cycle" of mud mounds. Such temporal constraints are essential to understand the dynamic processes and to identify forcing mechanisms and external controls.

2. Geological Setting

[4] The Central American Volcanic Arc (CAVA) extends from Panama in the south to Guatemala in the north and results from the subduction of the Cocos plate beneath the Caribbean plate [e.g., *Mann et al.*, 2007]. The CAVA is one of the most volcanically active regions in the world and produced numerous plinian eruptions in the last several hundred thousand years, which deposited tephra layers in the Pacific Ocean. Variations in the nature of the incoming plate [*Hoernle et al.*, 2002], in crustal thickness and composition [*Carr*, 1984] and in geophysical subduction parameters [*Syracuse and Abers*, 2006; *von Huene et al.*, 2000], caused systematic along-arc variations in

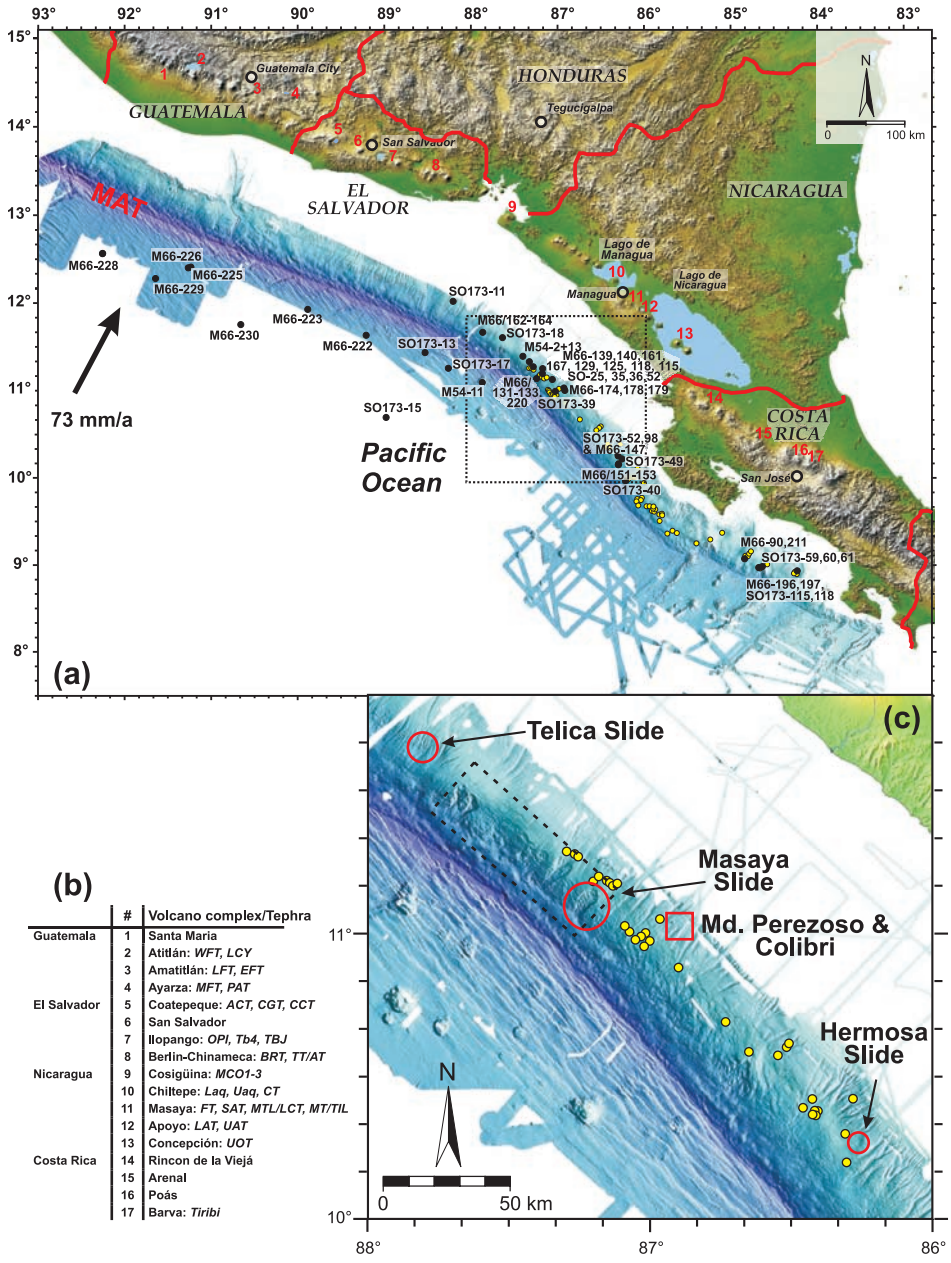

Figure 1. (a) Shaded and colored SRTM elevation model of Central America (NASA/JPL/NGA, 2000) and high-resolution bathymetry along the Middle America Trench (MAT) from *Ranero et al.* [2005]. The line of Central American arc volcanoes runs through the two large Nicaraguan lakes and parallel to the trench at 150–210 km distance. Black dots show core positions of R/V *METEOR* cruises M66 and M54 and R/V *SONNE* cruise SO173 along and across the trench. Yellow dots show distribution of methane seeps associated with mound and scar structures mapped at the slope offshore Costa Rica and Nicaragua by *Ranero et al.* [2008]. (b) Names of numbered volcanoes and major tephras: WFT, W-fall Tephra; LCY, Los Chocoyos Tephra; LFT, L-fall Tephra; EFT, E-fall Tephra; MFT, Mixta Tephra; PAT, Pinos Altos Tephra; ACT, Arce Tephra; CGT, Congo Tephra; CCT, Conacaste Tephra; OPI, Older pumice Ilopango; TB4, Terra Blanca 4 Tephra; TBJ, Terra Blanca Joven Tephra; BRT, Blanca Rosa Tephra; TT/AT, Twins/A-fall Tephra; MCO1-3, Mafic Cosigüina tephras; Laq, Lower Apoyeque Tephra; Uaq, Upper Apoyeque Tephra; CT, Chiltepe Tephra; FT, Fontana Tephra; SAT, San Antonio Tephra; MTL/LCT, Masaya Triple Layer/La Concepción Tephra; MT/TIL, Masaya Tuff/Ticuantepe Lapilli; LAT, Lower Apoyo Tephra; UAT, Upper Apoyo Tephra; UOT, Upper Ometepe Tephra. (c) Enlarged map section indicating landslides (red circles) and mud mounds (yellow dots) on the continental slope. Red rectangle gives position of Figure 5; black dashed rectangle gives position of Figure 3.

the composition of the volcanic rocks [*Carr et al.*, 2003, 2007; *Carr*, 1984; *Feigenson and Carr*, 1986; *Feigenson et al.*, 2004; *Hoernle et al.*, 2002; *Patino et al.*, 1997, 2000] that are very useful for geochemical correlations [*Kutterolf et al.*, 2008a].

[5] While bending into the subduction zone, the Cocos plate forms an outer rise in front of the trench along which it become dissected by numerous, deep-reaching bend faults [*Ranero et al.*, 2003]. Anomalous heat flow and seismic velocities indicate substantial hydration of crust and uppermost mantle by seawater invading the faults [*Grevemeyer et al.*, 2005], which is thought to be a major process to carry water into the subduction zone to ultimately generate melting in the mantle wedge [*Rüpke et al.*, 2002]. As the Cocos plate subducts beneath the Caribbean plate, the forearc is tectonically eroded [*Clift et al.*, 2005; *Ranero and von Huene*, 2000; *Vannucchi et al.*, 2004; *von Huene et al.*, 2004a]. Subduction erosion controls the structure of the forearc and causes oversteepening and destabilization of the continental slope particularly where seamounts are subducted [*von Huene et al.*, 2004b]. Parallel to the trench at intermediate water depths, the Middle American forearc is straddled with numerous fluid venting structures (Figure 1) believed to be fed by fluids expelled from subducted sediments by compaction and ascending along faults [*Hensen et al.*, 2004; *Moerz et al.*, 2005a, 2005b]. These include mud and carbonate mounds as well as vents at landslide scarps formed either by seamount subduction or by gas hydrate dissolution.

2.1. Mud and Carbonate Mounds

[6] Mud or carbonate mounds offshore Central America have diameters in the range of 100–2000 m and elevations above the surrounding seafloor of 20–200 m. They are composed of over-consolidated mud clasts, liquefied mudflows as well as highly variable authigenic carbonates. Mounds are mostly covered by massive carbonate crusts and boulders formed by the anaerobic oxidation of methane at the seafloor and in the extruded sediments [*Moerz et al.*, 2005b]. Seismic profiles show that the mounds visible at the surface cap are diatreme structures dissecting the gas hydrate layer (visible as Bottom Simulating Reflector, BSR) and extending at least several hundred meters deep into the forearc [*Talukder et al.*, 2007]. Fluid-chemical (Cl-depleted pore waters, C-isotopes) and petrographic evidence (MORB fragments, over-consolidated clay clasts) show that the fluids probably derive from dewatering of subducted sediments at 10–15 km depth, using permeable forearc faults created by tectonic erosion [*Ranero et al.*, 2008] to ascend to the surface [*Grevemeyer et al.*, 2004; *Hensen et al.*, 2004; *Mau et al.*, 2006, 2007; *Moerz et al.*, 2005a, 2005b]. The methane output flux at vent structures is temporally variable [*Mau et al.*, 2006]. Typically mixed sediments occur around mound structures that are thought to have been ejected during phases of intense activity [*Moerz et al.*, 2005b]. Their intercalation with background pelagic sediments demonstrates that mound activity is not steady but periodic. However, the lifetime of mud mounds and the age and duration of active periods are presently unknown.

2.2. Submarine Slides

[7] The sedimentary architecture of active and passive continental margins is frequently modified by submarine slope failures, which can occur on larger scales than known from terrestrial mass wasting events. Volumes of up to 20000 km^3 (e.g., Agulhas slide [*Hampton et al.*, 1996]) are mobilized, probably in a catastrophic manner, and are therefore a potential trigger mechanism for tsunamis that can devastate coastal areas [*Tappin et al.*, 2001]. The formation of gas hydrates cements and stabilizes the slope sediments but also prevents further compaction and build-up of shear strength [*Reston and Bialas*, 2002]. Partial dissolution of gas hydrates thus favors the formation of submarine landslides that may be triggered by earthquakes, particularly on continental slopes steepened by subduction erosion [*Harders et al.*, 2006]. Two different types of slope failure have been identified on the continental slope off Costa Rica and Nicaragua: rotational slumps and translational slides. Rotational slumps appear to be triggered by seamount subduction [*von Huene et al.*, 2000, 2004b]. In contrast, the formation of translational slides appears to be related to layers of low shear strength in the sediment succession [*Harders et al.*, 2006].

3. Marine Sediment Cores

3.1. Marine Core Sampling

[8] During R/V *METEOR* cruises M54/2 and M66/3 as well as R/V *SONNE* cruise SO173/3, 56 sediment gravity cores have been collected offshore Central America. The locations (9°12′N/

84°39′E and 12°45′N/92°30′E) of the cores are on the oceanic plate and the continental slope in 1200–4000 m water depth and distances of 150–370 km from the CAVA (Figure 1). The cores contain 213 ash horizons including primary ash layers and slightly reworked ash that retained its compositional integrity and stratigraphic position and therefore can be used as marker beds. Criteria identifying primary and variably reworked ash horizons, and the methods employed to correlate them with deposits on land are described and discussed in part 1 [*Kutterolf et al.*, 2008a]. In the following we focus on the intercalated sediments and on cores from sites that have been specifically targeted to penetrate sediments at mound structures, landslide deposits, and landslide detachment planes.

3.2. General Description of Cores

[9] The 56 cores collected from offshore Central America contain a total of 213 ash bearing horizons, including 133 distinct ash layers. Of these, 69 are light gray to white felsic ashes, 24 are gray layers of intermediate composition and 40 are black mafic layers. The ash layers and their components are described in more detail in part 1 of this contribution [*Kutterolf et al.*, 2008a].

[10] Pelagic silty to sandy clay sediment is commonly dark olive green but changes to lighter shades of green deeper in the cores. The pelagic sediment is mixed with terrigeneous input from the volcanic arc and its basement. The modal composition is typically 10 to 20% total quartz, 40 to 60% of clay (mainly smectite), 20 to 30% feldspar, and fresh to incipiently altered volcanic glass shards and rock fragments of various compositions (reworked sediments, basalts, carbonates). Additionally, <10% pyrite, 10 to 20% biogenic material including foraminifers, diatoms, some radiolarians and occasionally slope detritus like shells and corals can be found in the cores. Accessory chlorite clasts (<2%) occur in nearly every examined sample.

[11] In the upper part of core M66-228, M54-11, SO173-17, lower part of SO173-15, 18 and M54-13, and the entire sections of M66 cores 222 and 229, the pelagic sediment is compositionally and structurally completely monotonous indicating continuous sedimentation at constant rates. In other cores and core sections, however, there are abundant structural indications of small-scale slumping and mingling events interrupting the background clay sedimentation, even in cores from the incoming plate at considerable distance from the trench axis. This local small-scale reworking, however, did not significantly affect the stratigraphic order of the ash horizons.

[12] Sediment successions at the carbonate and mud mounds differ by including layers compositionally dominated by the products of these structures. Color changes from dark-olive-green to light-olive-gray of the fine grained matrix reflect increasing abundance of carbonate mud derived from the active mound. The clast components in the lighter layers are dominated by carbonate and/or mud detritus including over-consolidated "scaly" clay clasts that originated from deeper levels. Such layers are interpreted as mudflow deposits emitted by mud volcanoes [*Moerz et al.*, 2005a, 2005b]. During inactive phases of the mounds, the background clay sedimentation continues. At the intermediate depths on the slope, these sediments are heterogeneous and include abundant detritus from the shelf such as fragments of oysters, corals, and wood.

4. Applications of Tephrostratigraphy to Continental Slope Geology

[13] We focus on the Pacific region offshore Nicaragua. Table 1 summarizes a subset of 22 of the tephras correlated in part 1 that are relevant for the determination of ages and rates of the geological processes discussed in the following. These 22 tephras have well-constrained ages, characteristic compositions and form distinct distal marine ash beds.

4.1. Sedimentation Rates

[14] Time marks given by dated ash layers allow us to calculate average apparent sedimentation rates of the intercalated pelagic sediment (Figure 2, Figure S1[1], and Table 1). In these calculations, the thickness of the intercalated sediment interval is reduced by the intervening undated ash beds to obtain the pelagic sediment thickness. However, the pelagic clay is often mixed to variable extent with volcanic ash particles, which contribute to the sedimentation rate but are not corrected for. Sediment-petrographic studies underway will further refine sedimentation rates. Some core sections show intense bioturbation and the addition of organic matter may have increased the sediment

[1] Auxiliary materials are available in the HTML. doi:10.1029/2007GC001826.

Table 1. Summary of 22 Onshore Tephras Correlated in Part 1 That Are Relevant for the Determination of Ages and Rates of the Geological Processes[a]

Tephra Name	Tephra Acronym	Correlated Ash Layers	Age, ka	Source Volcano	Country	Max. Observed Ash Dispersal From the Source, km
Tierra Blanca Joven Tephra	TBJ	C1	1.6	Ilopango Caldera	El Salvador	390
Masaya Tuff/Ticuantepe Lapilli	MT/TIL	C2	1.8	Masaya Caldera	Nicaragua	200
Chiltepe Tephra	CT	C3	1.9	Chiletepe complex	Nicaragua	570
Masaya Triple Layer/ La Concepción Tephra	MTL/LCT	C4	2.1	Masaya Caldera	Nicaragua	170
San Antonio Tephra	SAT	C5	6	Masaya Caldera	Nicaragua	330
Upper Apoyeque Tephra	UAq	C6	12.4	Chiletepe complex	Nicaragua	300
Lower Apoyeque Tephra	LAq	C7	17	Chiletepe complex	Nicaragua	210
Upper Ometepe Tephra	UOT	C8	19	Concepción volcano	Nicaragua	280
Mafic Cosigüina Tephras	MCO	C9	21–23	Cosigüina volcano	Nicaragua	220
Upper Apoyo Tephra	UAT	C10	24.5	Apoyo Caldera	Nicaragua	530
Lower Apoyo Tephra	LAT	C11	24.8	Apoyo Caldera	Nicaragua	270
Tierra Blanca 4 Tephra	TB4	C12	36	Ilopango Caldera	El Salvador	380
Mixta Fall Tephra	MFT	C13	39	Ayarza Caldera	Guatemala	340
Conacaste Tephra	CCT	C14	51	Coatepeque Caldera	El Salvador	320
Congo Tephra	CGT	C15	53	Coatepeque Caldera	El Salvador	320
Fontana Tephra	FT	C16	~60	Las Nubes Caldera	Nicaragua	330
Twins/A-Fall Tephra	TT/AT	C17	60	Berlin-Pacayal-Volcan group	El Salvador	270
Arce tephra	ACT	C18	75	Coatepeque Caldera	El Salvador	320
Older Ilopango Pumice	OPI	C20	75–84	Ilopango Caldera	El Salvador	470
Los Chocoyos tephra	LCY	C21	84	Atitlán Caldera	Guatemala	1900
W-Fall Tephra	WFT	C22	158	Atitlán Caldera	Guatemala	560
L-Fall Tephra	LFT	C23	191	Amatitlán Caldera	Guatemala	810

[a] Ash layers (C#) were correlated by *Kutterolf et al.* [2008a].

thickness. Also, we typically obtain higher apparent sedimentation rates for the upper few decimeters of the cores than for deeper levels due to incomplete compaction near the seafloor. Since we do not attempt to correct for compaction, this must be considered when comparing apparent sedimentation rates for different age intervals.

[15] In general, we observe pelagic sedimentation rates of ~1–6 cm/ka on the incoming plate and up to 30–40 cm/ka on the continental slope. However, the apparent sedimentation rates vary with depth in the cores and between cores, both at the continental slope and on the incoming plate. In core SO173-15 at a position farthest away from the trench on the incoming plate (Figure 1), the apparent sedimentation rate gradually decreases with depth (Figure 2a). The high value of 27.5 cm/ka near the top reflects the poor compaction of the sediment. Below ~60 cm bsf, the sedimentation rate rapidly decreases to 5.7 cm/ka, similar to the 5.4 cm/ka estimated by *Bowles et al.* [1973]; this may be taken as a representative value of monotonous sedimentation on the Cocos plate offshore Nicaragua.

4.2. Sedimentation and Bend Faulting

[16] Sedimentation was not monotonous everywhere on the incoming plate. In core M66-222 (Figure 1; see Figure 10 in part 1), ash layers C10 (distal ash of the 24.5 ka Upper Apoyo Tephra, UAT) and C15 (53 ka Congo Tephra, CGT) are separated by ~188 cm of pelagic sediment indicating an average accumulation rate of 6.7 cm/ka. In contrast, ash bed C10 immediately follows atop ash pods of C15 in core M66-230; apparently some erosive event has removed sediment accumulated above C15 prior to emplacement of C10. Another example is core SO173-17 on the incoming plate offshore Nicaragua (Figure S1) where ash layers C10 (UAT) and C11, the distal ash of the Lower (LAT) Apoyo tephra, are separated by 15 cm sediment such that the sedimentation rate of 2 cm/ka determined by other ash beds implies a time period of ~7 ka between these eruptions. Geological evidence on land and overlapping radiocarbon ages [*Kutterolf et al.*, 2007a] demonstrate these eruptions occurred within a few hundred years at around 25 ka. Moreover, LAT and UAT are separated by 7 cm sediment on the continental slope

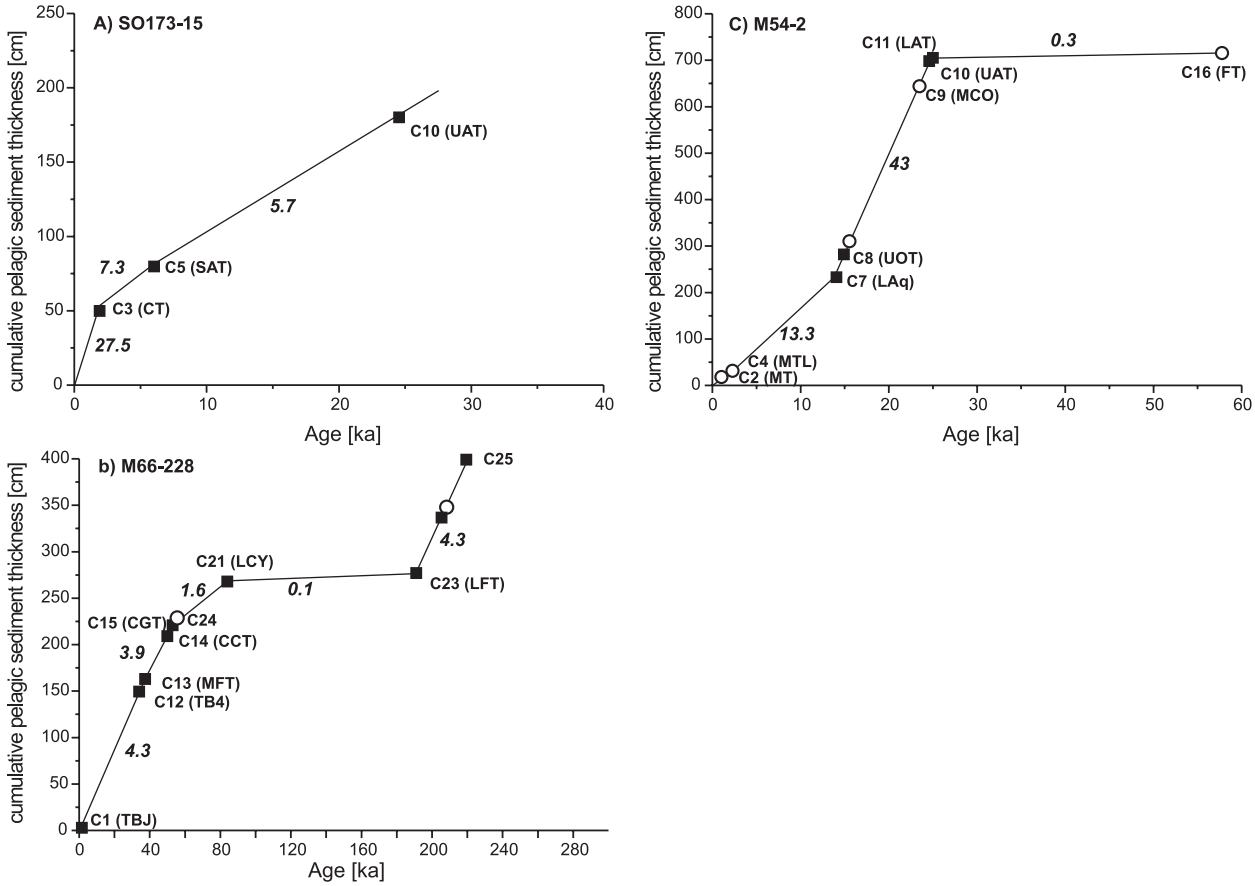

Figure 2. Cumulative thickness of pelagic sediment versus age for selected cores. (a) Core SO173-15 on incoming plate ~200 km distance from the trench. (b) Core M66-228 on incoming plate close to the trench; C25 only correlated to marine cores, not to tephras on land. (c) Core M54-2 on the middle continental slope. Filled squares show felsic ash layers and white circles show mafic ash layers correlated to field tephras (see Figure 1 for acronyms) of known age after *Kutterolf et al.* [2008a]. The slopes of line segments between tephras yield average apparent accumulation rates (numbers in cm/ka). Respective diagrams for other cores are shown in auxiliary material Figure S1.

(core M54-2; Figure 2c), where accumulation at 43 cm/ka suggests a time interval of ~200 years. The sediment interval in core SO173-17 contains small ash lenses of underlying LAT ash indicating that its excess thickness is due to reworking.

[17] Anomalously low apparent sedimentation rates of mostly <1 cm/ka mark the time intervals of 50–190 ka in core M66-223, 60–160 ka in core M66-230, 90–190 ka in cores M66-226 and M66-228 (Figure 2b), and to lesser extent at 60–70 ka in core M66-229 (Figure S1). Lower apparent sedimentation rates are also found at around 200 cm depths, or at >80 ka age, in cores SO173-17 and M54-11 closer to the trench offshore Nicaragua (Figure S1). These dramatic reductions in apparent sedimentation rate are not related to compaction because they occur at a similar age range but at different depths in the cores, e.g., beginning at 60 cm depth bsf in cores M66-223 and M66-226 but at 270 cm depth in core M66-229. Moreover, pore water analyses and strength measurements as well as core-logging data did not reveal significant differences in the state of sediment compaction (T. Mörz, personal communication, 2006). Structures such as clay lenses (see Figure 3e in part 1) and tilted ash pods rather suggest that the low apparent sedimentation rates result from repeated small-scale erosive events that occurred on the incoming plate. Although some turbidity currents from the continental slope may have reached the drill sites on the incoming plate, these were probably no longer erosive after crossing the trench and climbing the outer rise. We rather interpret that these local events of erosion and reworking were related to tectonic activity at the numerous bend faults that dissect the incoming plate on the outer rise and

have offsets increasing toward the trench (Figure 1) [*Ranero et al.*, 2005]. During the time span represented by the cores, core positions moved about 30 km along the subduction vector but remained within the zone of bend faulting. Across <50 ka sections of the cores, sedimentation rates are higher but laterally variable. Apparent sedimentation rates of 4–7.5 cm/ka in cores M66-228 and M66-229 farther away from the trench contrast with 0.6 and 1.1 cm/ka in cores M66-226 and M66-223 closer to the trench where fault offsets are larger. This suggests a tendency for stronger sediment reworking where fault offsets are larger. On the other hand, core M66-222 with 6.7 cm/ka is also close to the trench while core M66-230 with only 4.2 cm/ka lies farther away. Hence the local sedimentation and erosion of the younger core sections is controlled by both distance from trench (magnitude of fault offset) and proximity to the local faults (unknown due to insufficient resolution of core positioning and bathymetry). The apparent sedimentation rates of the older core sections are significantly lower but much more uniform between cores. A possible explanation may be that one or more intense tectonic events occurred between 80–190 ka that caused dramatic regional erosion irrespective of the detailed core position. An implication of this interpretation is that bend faulting is not continuous but proceeds by sporadic bursts that are separated by periods of less intense activity lasting on the order of 10^4 years.

4.3. Sedimentation on the Continental Slope

[18] Cores from the continental slope offshore Nicaragua reveal large differences in apparent sedimentation rates at comparable time intervals. For example, the core M54-2 (Figure 2c) has ~4 m sediment between ash layers C7 (LAq) and C10 (UAT), yielding accumulation at 35 cm/ka, while this interval is condensed to only ~0.2 m (2.2 cm/ka) in neighboring core M54–13 (Figure 1). The sediment thickness between layer C4 (2.1 ka MTL) and C7 is more than halved from core SO173-18 to M54-2. The top section above C2 (1.8 ka MT) likewise reduces from 1.5 m to 10 cm (rate from 90 to 13.3 cm/ka). The accumulated sediment of the past 6 ka is strongly reduced (1.1 cm/ka sedimentation rate) at the top of M54-13. These comparisons show that there are large local and temporal deviations from the "normal" accumulation rate of 30–40 cm/ka estimated from other, more monotonous cores (Figure S1). We interpret that these variations in apparent accumulation rates reflect laterally and temporally variable phases of excess sediment delivery and erosion probably by turbidity currents descending the slope. For example, excess accumulation rate of ~90 cm/ka across the upper 1.5 m of core SO173-18, which was taken from the rim of a submarine canyon on the Nicaraguan slope (Figure 1), can be explained by accumulation of turbidite overbank sediments from currents passing through the canyon.

[19] On land in Nicaragua we have identified major periods of erosion that occurred around 17–25 ka and 2–6 ka (unconformities U1 and U2-4 [*Kutterolf et al.*, 2007a]). Increased turbidity current activity on the continental slope causing lateral changes in apparent accumulation rates is probably linked to these erosive phases on land which appear to be related to tectonic activity (U1) and changing climatic conditions (U2-4) [*Kutterolf et al.*, 2007a]. There is no evidence on land correlating with erosion on the continental slope during the past <2 ka seen in some cores; this seems to be controlled by conditions at the slope only. We note that this is a preliminary interpretation because detailed petrographic studies of the sediments still need to be done. The absence of sharp unconformities in condensed sections can be explained by reworking of the soft sediments in an unconsolidated state.

4.4. Submarine Landslides and Ash Layers

[20] Fast, erosive subduction of the rough Cocos Plate beneath the Caribbean Plate leads to an oversteepening of the Nicaraguan continental slope [*Ranero and von Huene*, 2000; *von Huene et al.*, 2004b] on which sediment packages become unstable and collapse as submarine landslides [*Harders et al.*, 2006]. Large failures are abundant on the middle slope offshore Nicaragua (Figure 3) and increase the tsunami hazard. Detachment planes of landslides typically form in sediment layers of low shear strength. Drilling through two exposed slide planes offshore Costa Rica (SO173-59) and Nicaragua (M66/3-151) showed that detachment occurred at the level of ash layers. We use core M66/3-151 from the Hermosa slide as an illustrative example. An unconformity at 1.5 m bsf separates overlying undisturbed massive homogeneous pelagic clay from underlying, <10-cm-thick reworked mélange containing rounded intraclasts of consolidated clay in an unconsolidated clay matrix mixed with ash. This is underlain by a mafic ash layer that has an eroded top and high

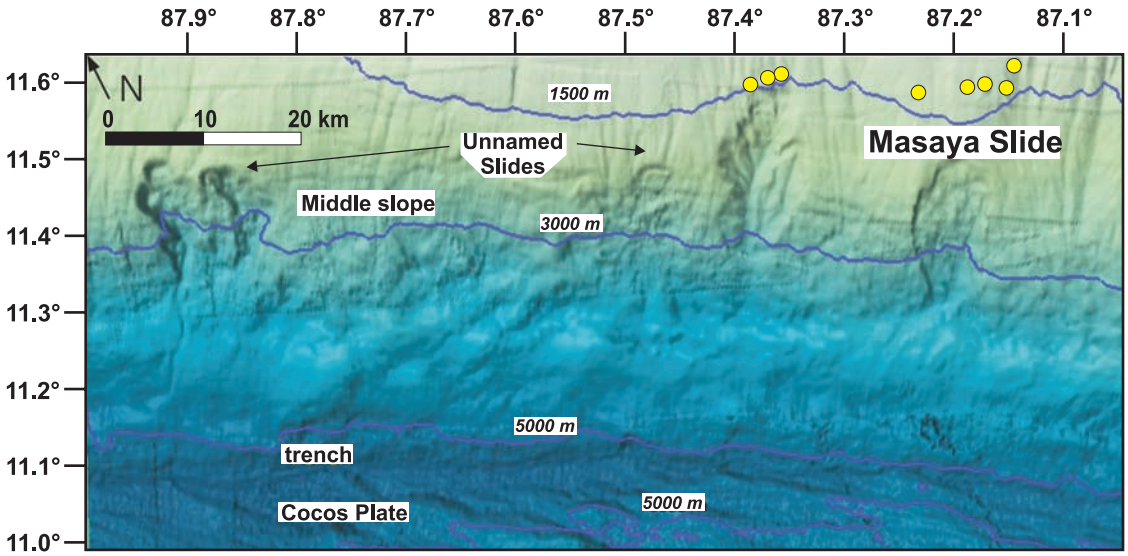

Figure 3. Bathymetric map of the middle slope offshore central Nicaragua (see Figure 1c) showing slide scarps that have dimensions from several kilometers up to tens of kilometers, and headwalls up to 100 m high. Yellow circles show fluid vents above the Masaya Slide.

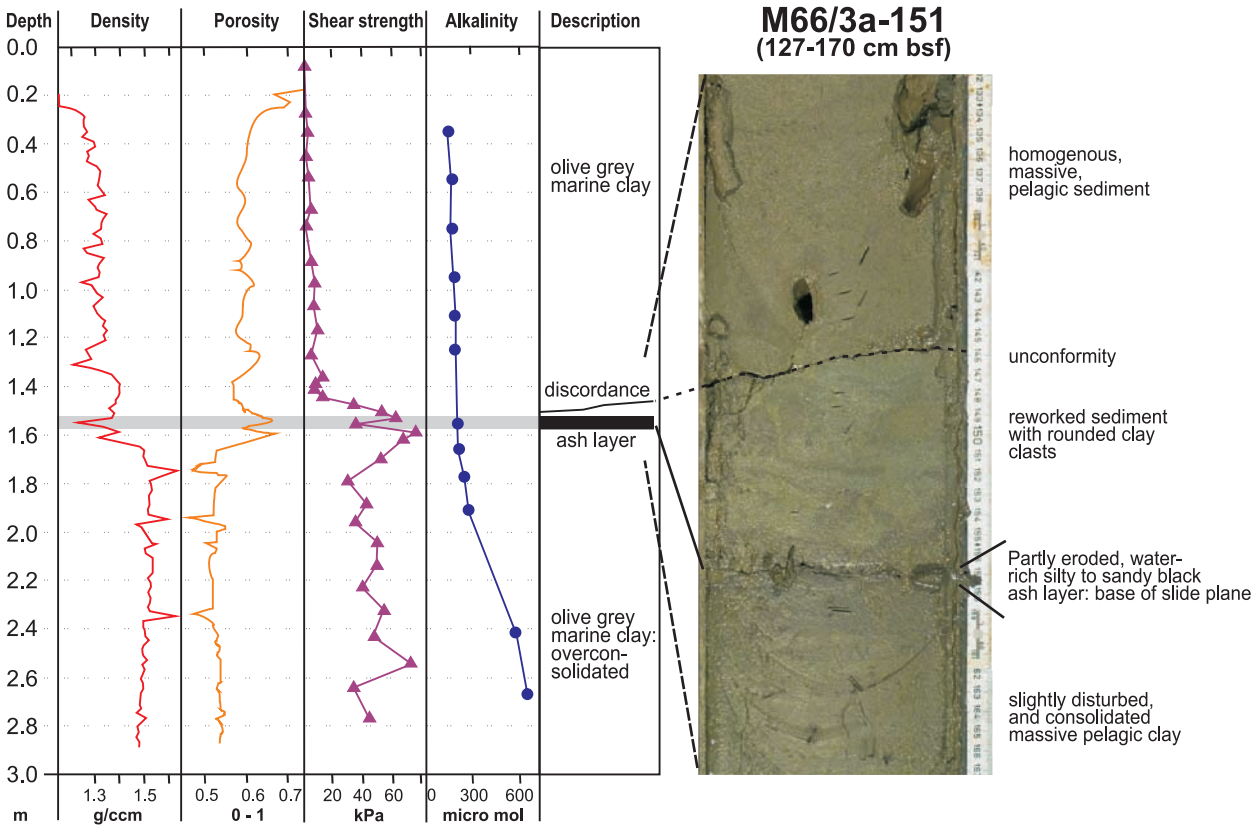

Figure 4. Physical and geochemical logging parameters of core M66/151 drilled through the detachment plane of the Hermosa slide (Figure 1c). The core section photograph shows the slide plane covered by a mafic ash layer of low shear strength that is overlain by 10 cm of clay mélange which is capped by the upper detachment unconformity.

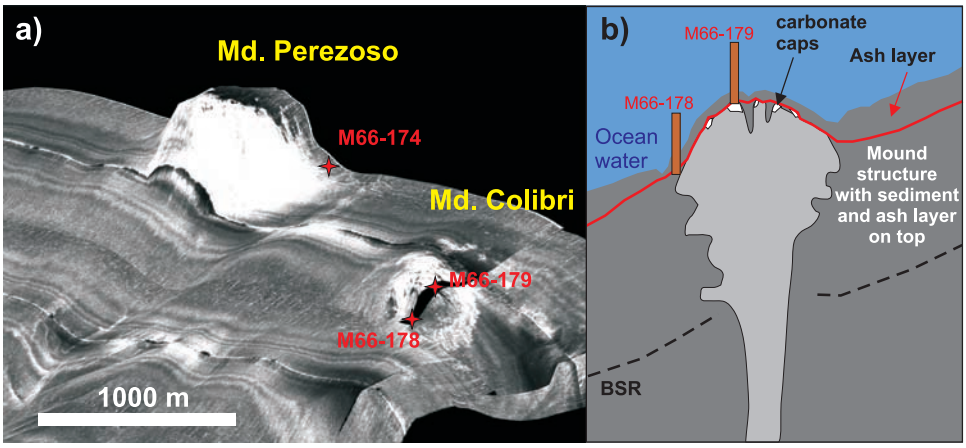

Figure 5. (a) Side-scan sonar backscatter image of Mounds Colibri and Perezoso with gravity core positions (red diamonds and labels); 3 times vertical exaggeration. The dimensions (height/length/width) of the structures are 130/940/780 m for Perezoso and 30/620/588 m for Colibri. (b) Schematic cross section of a mound structure overlain by an ash layer (modified after *Moerz et al.* [2005a]) showing the core positions M66-178 on the lower flank and M66/179 on the top. BSR is Bottom Simulating Reflector, marking the base of the gas hydrate layer interrupted by mud diapirism.

porosity and low density in the core logging data (Figure 4). The massive clay below the ash layer is slightly deformed near the top. Low porosity, high density and high pore water alkalinity show that this lower clay package is significantly more compacted and older than the clay package above the unconformity. Measured shear strength decreases steeply from high values in the underlying clay to low values in the clay overlying the unconformity (Figure 4). The steep gradients in physical properties and residence time (alkalinity) and the deformation structures strongly suggest that a significant sediment package has been removed from this level by sliding prior to renewed pelagic sedimentation above the unconformity. The shear zone of detachment reaches from the unconformity to the ash layer but minor shear also affected the top of the underlying clay. Within the steep shear strength gradient across this zone, the ash layer marks an excursion to about half the strength value. Moreover, the high porosity of the well-sorted ash and its being sealed by impermeable clay at top and bottom suggests that high pore pressure would have been generated in the ash layer during compaction, further reducing its strength. Ash layers thus are predestined to form structurally weak horizons on which sediment packages begin to slide when triggered by processes such as steepening of the slope.

[21] The mafic ash layer in the detachment zone of the Hermosa slide correlates with the ~6 ka old San Antonio Tephra erupted from Masaya Caldera [*Kutterolf et al.*, 2007a; *Pérez and Freundt*, 2006]. The slide detachment thus occurred less than 6 ka ago. Core M66/3-162 penetrated the detachment plane of the Telica slide, which is overlain by the distal ash of the ~60 ka Fontana Tephra at 57–59 cm bsf such that the landslide occurred more than 60 ka ago. The Masaya slide, the largest known landslide offshore Nicaragua, occurred ~19 ka ago because its detachment plane is immediately overlain by distal ashes of the ~17 ka Lower Apoyeque and ~19 ka Upper Ometepe tephras in cores M66/3-132 and 220. These examples illustrate how useful marine ash layers are to constrain ages of submarine landslides provided they can be correlated to tephras of known age or otherwise dated.

4.5. Dating Mud-Mound Activity by Ash Layers

[22] Mud-mound formation processes are discussed in detail by [*Moerz et al.*, 2005a, 2005b]. Mud mounds evolve unsteadily and their surrounding sediments provide a record of alternating active and inactive phases. We use Mound Colibri offshore central Nicaragua (Figure 1) as an illustrative example. The side-scan sonar backscatter image (Figure 5a) shows Mound Colibri and adjacent Mound Perezosa rising above the seafloor and capped by highly reflective carbonate. These structures have dimensions typical of mounds offshore Nicaragua which range from several tens of meters to hundreds of meters height and from 0.2 to

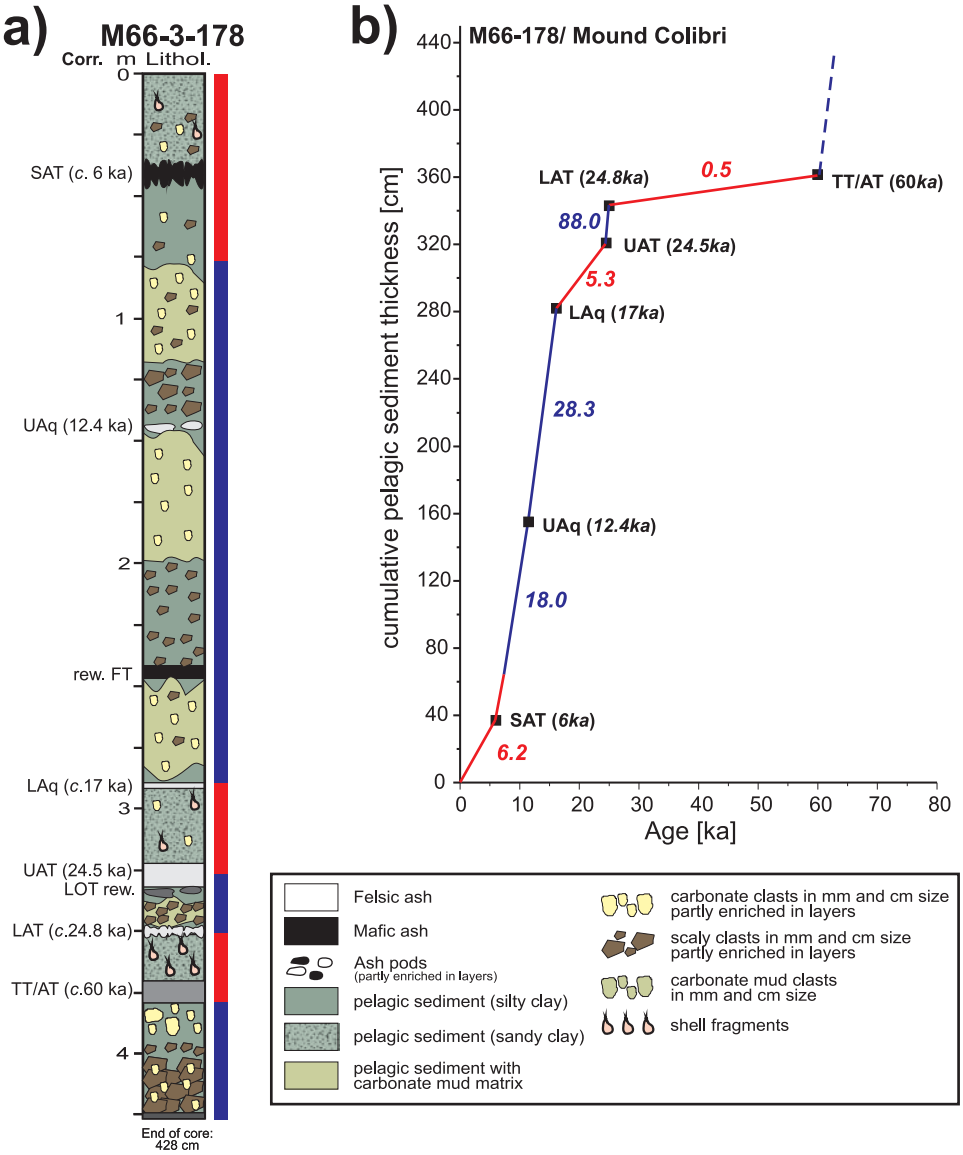

Figure 6. (a) Lithologic section of core M66-178 with correlated ash layers. SAT, 6 ka San Antonio Tephra; UAq, 12.4 ka Upper Apoyeque Tephra; LAq, ~17 ka Lower Apoyeque Tephra; UAT, 24.5 ka Upper Upoyo Tephra; LAT, 24.8 ka Lower Apoyo Tephra; TT/AT, ~60 ka Twins/A-fall Tephra. Blue bars along section mark intervals of mound sediments; red bars mark pelagic background sediments. (b) Cumulative pelagic sediment thickness versus age. Squares mark correlated ash layers of known age. Line slopes give apparent sedimentation rates (numbers in cm/ka) varying along the core. Blue line segments mark mud-mound activity; red line sections mark phases of relative inactivity.

>1.0 km^2 basal area. Such visible dimensions, however, have no relation to the age of the cold seep structures (D. Bürk, personal communication, 2007). Core M66/3-178, drilled through the flank of Mound Colibri, contains two major types of sediment (Figure 6a): (1) rounded clay and carbonate clasts, ash lenses and shelf-derived fossils dispersed in a matrix of sandy clay and (2) a bimodal population of angular scaly clay and carbonate clasts in a fine-grained matrix of clay or carbonate mud. The inventory of sediment (2) is the typical material ejected by mound structures during phases of strong venting activity [*Moerz et al.*, 2005b]. The heterolithologic sediment (1) typical of the background sedimentation on the middle slope receiving input from the shelf is emplaced while the adjacent mound was relatively inactive. The sediments in core M66/3-178

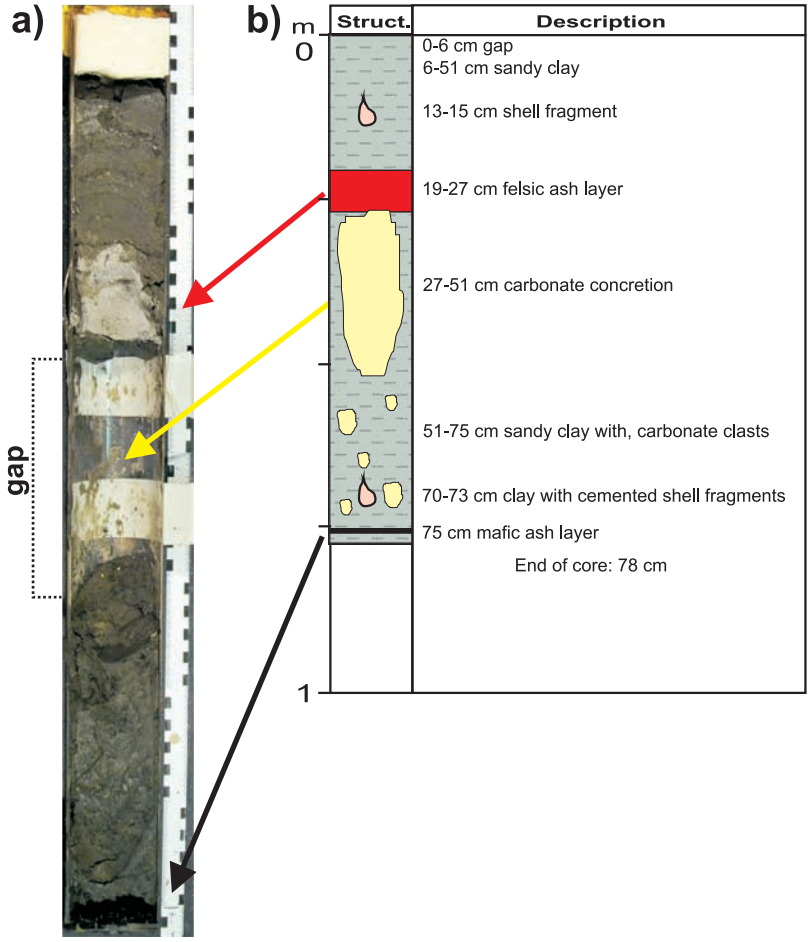

Figure 7. (a) Core M66-179 section 0–100 cm bsf obtained by vibrocorer shows a white marine ash layer (24.5 ka UAT) atop a carbonate concretion at the top of Mound Colibri. The carbonate section of 30 cm thickness was removed to facilitate opening of the core. (b) Description of the core section shown in Figure 7a.

are intercalated with ash layers that we correlate with dated tephras on land. These time constraints show that apparent sedimentation rates are strongly elevated above background levels at intervals composed of type-2 mound sediments (Figure 6b). The ash layers show that Mound Colibri had at least three phases of high venting activity at >60 ka, a short phase at 24.5–24.8 ka, and an extended phase from 17 to ~8 ka.

[23] Core M66/3-179 drilled on the top of Mound Colibri contains distal ash of the 25 ka Upper Apoyo Tephra above the carbonate cap and overlain by pelagic sediment type-1 (Figure 7). This would suggest mound activity terminated >25 ka ago in contrast to the above results from core M66/3-178 from the mound flank. This discrepancy may be due to erosion at the mound top or to lateral shifting of vents across the mound; in any case, this example suggests that flank cores are more useful to decipher an extended history of mound activity. These preliminary results, which for the first time provide absolute ages for active mud mound phases, demonstrate the power of marine tephrostratigraphy in understanding the periodic dynamic evolution of mud mounds.

5. Conclusions

[24] Apart from helping to reconstruct the history of arc volcanism, offshore tephrostratigraphy also delivers important data for understanding geological processes operating at the continental slope and on the incoming plate. Apparent pelagic sedimentation rates derived from dated ash layers identify periods of erosion and enhanced accumulation both at the continental slope, where they seem to be related to climatic and possibly tectonic conditions on land, and on the incoming plate,

where they are related to bend faulting of the plate across the outer rise.

[25] Dated ash layers also constrain the times at which submarine landslides detached from the continental slope; such slides often used ash beds as low-strength shear planes. Moreover, using correlated ash layers, we were able for the first time to determine the age and duration of repeated phases of high venting activity alternating with periods of low or no activity of mud mounds.

Acknowledgments

[26] We especially thank all members of the scientific parties of R/V *METEOR* cruises M66/3 and M54/2 and R/V *SONNE* cruise SO173/3 for the good and successful working atmosphere. Eric Steen and Mark Schmidt did the coring. We also thank Oliver Bardtoff, Cosima Burkert, Kristina Bernoth, Emelina Cordero, Joana Deppe, Yann Lahaye, Julia Mahlke, Dagmar Rau, and Mario Thöner, who assisted sampling on board, sample preparation, and analytical work. W.P. acknowledges a Ph.D. stipend by the Deutscher Akademischer Austauschdienst (DAAD). We also appreciate the helpful comments and suggestions of Vincent Salters, Stephen Blake, Mike Carr, Phil Shane, and Tom Vogel, who reviewed an earlier version of this paper. This publication is contribution 106 of the Sonderforschungsbereich 574 "Volatiles and Fluids in Subduction Zones" at Kiel University. R/V *METEOR* and R/V *SONNE* cruises were funded by the Deutsche Forschungsgemeinschaft (DFG).

References

Bowles, F. A., R. N. Jack, and I. S. E. Carmichael (1973), Investigation of deep-sea volcanic ash layers from equatorial Pacific cores, *Geol. Soc. Am. Bull.*, *84*, 2371–2388.

Carr, M., M. D. Feigenson, L. C. Patino, and J. A. Walker (2003), Volcanism and geochemistry in Central America: Progress and problems, in *Inside the Subduction Factory*, *Geophys. Monogr. Ser.*, vol. 138, edited by J. Eiler, pp. 153–174, AGU, Washington, D. C.

Carr, M. J. (1984), Symmetrical and segmented variation of physical and geochemical characteristics of the Central American Volcanic Front, *J. Volcanol. Geotherm. Res.*, *20*, 231–252.

Carr, M. J., L. C. Patino, and M. D. Feigenson (2007), Petrology and geochemistry of lavas, in *Central America—Geology, Resources and Hazards*, vol. 2, edited by J. Buntschuh and G. E. Alvarado, pp. 565–590, A. A. Balkema, Rotterdam, Netherlands.

Clift, P. D., L.-H. Chan, J. Blusztajn, G. D. Layne, M. Kastner, and R. K. Kelly (2005), Pulsed subduction accretion and tectonic erosion reconstructed since 2.5 Ma from the tephra record offshore Costa Rica, *Geochem. Geophys. Geosyst.*, *6*, Q09016, doi:10.1029/2005GC000963.

Feigenson, M. D., and M. J. Carr (1986), Positively correlated Nd and Sr isotope ratios of lavas from the Central American volcanic front, *Geology*, *14*, 79–82.

Feigenson, M. D., M. J. Carr, S. V. Maharaj, S. Juliano, and L. L. Bolge (2004), Lead isotope composition of Central American volcanoes: Influence of the Galapagos plume, *Geochem. Geophys. Geosyst.*, *5*, Q06001, doi:10.1029/2003GC000621.

Grevemeyer, I., A. Kopf, N. Fekete, N. Kaul, M. Heesemann, H.-H. Gennerich, M. Müller, V. Spiess, K. Wallmann, and W. Weinrebe (2004), Fluid flow trough active mud dome Mound Culebra offshore Nicoya Peninsula, Costa Rica: Evidence from heat flow surveying, *Mar. Geol.*, *207*(1–4), 145–157.

Grevemeyer, I., N. Kaul, J. L. Diaz-Naveas, H. W. Villinger, C. R. Ranero, and C. Reichert (2005), Heat flow and bending-related faulting at subduction trenches: Case studies offshore of Nicaragua and central Chile, *Earth Planet. Sci. Lett.*, *236*, 238–248.

Hampton, M. E., H. J. Lee, and J. Locat (1996), Submarine landslides, *Rev. Geophys.*, *34*, 33–59.

Harders, R., W. Brückmann, V. Feeser, C. Hensen, and S. Kutterolf (2006), Ash layers: The controlling factor on translational sliding offshore Central America?, *Eos Trans. AGU*, *87*(52), Fall Meet. Suppl., Abstract OS43C-0666.

Hensen, C., K. Wallmann, M. Schmidt, C. R. Ranero, and E. Suess (2004), Fluid expulsion related to mud extrusion off Costa Rica continental margin—A window to the subducting slab, *Geology*, *32*, 201–204.

Hoernle, K., P. van den Bogaard, R. Werner, B. Lissinna, G. E. Alvarado, and D. C.-Garbe-Schönberg (2002), Missing history (16–71 Ma) of the Galapagos hotspot: Implications for the tectonic and biological evolution of the Americas, *Geology*, *30*(9), 795–798.

Kutterolf, S., A. Freundt, W. Peréz, H. Wehrmann, and H.-U. Schmincke (2007a), Late Pleistocene to Holocene temporal succession and magnitudes of highly-explosive volcanic eruptions in west-central Nicaragua, *J. Volcanol. Geotherm. Res.*, *163*, 55–82.

Kutterolf, S., U. Schacht, H. Wehrmann, A. Freundt, and T. Mörz (2007b), Onshore to offshore tephrostratigraphy and marine ash layer diagenesis in Central America, in *Central America—Geology, Resources and Hazards*, vol. 2, edited by J. Buntschuh and G. E. Alvarado, pp. 395–423, A. A. Balkema, Lisse, Netherlands.

Kutterolf, S., A. Freundt, W. Peréz, T. Mörz, U. Schacht, H. Wehrmann, and H.-U. Schmincke (2008a), Pacific offshore record of plinian arc volcanism in Central America: 1. Along-arc correlations, *Geochem. Geophys. Geosyst.*, doi:10.1029/2007GC001631, in press.

Kutterolf, S., A. Freundt, and W. Peréz (2008b), Pacific offshore record of plinian arc volcanism in Central America: 2. Tephra volumes and erupted masses, *Geochem. Geophys. Geosyst.*, doi:10.1029/2007GC001791, in press.

Mann, P., R. D. Rogers, and L. Gahagan (2007), Overview of plate tectonic history and its unresolved tectonic problems, in *Central America—Geology, Resources and Hazards*, vol. 2, edited by J. Buntschuh and G. E. Alvarado, pp. 201–238, A. A. Balkema, Lisse, Netherlands.

Mau, S., H. Sahling, G. Rehder, E. Suess, P. Linke, and E. Soeding (2006), Estimates of methane output from mud extrusions at the erosive convergent margin off Costa Rica, *Mar. Geol.*, *225*, 129–144.

Mau, S., G. Rehder, I. G. Arroyo, J. Gossler, and E. Suess (2007), Indications of a link between seismotectonics and CH4 release from seeps off Costa Rica, *Geochem. Geophys. Geosyst.*, *8*, Q04003, doi:10.1029/2006GC001326.

Moerz, T., et al. (2005a), Styles and productivity of diapirism along the Middle America margin, Part II: Mound Culebra and Mounds 11, and 12, in *Mud Volcanoes, Geodynamics and Seismicity*, *NATO Sci. Ser., Ser. IV*, vol. 51, edited by G. Martinelli and B. Panahi, Springer, Dordrecht, Germany.

Moerz, T., A. Kopf, W. Brueckmann, H. Sahling, N. Fekete, V. Hühnerbach, D. Masson, D. A. Hepp, and E. Suess (2005b), Styles and productivity of diapirism along the Middle America margin, Part I: Margin evolution, segmentation, dewatering and mud diapirism, in *Mud Volcanoes, Geodynamics and Seismicity*, *NATO Sci. Ser., Ser. IV*, vol. 51, edited by G. Martinelli and B. Panahi, pp. 35–48, Springer, Dordrecht, Germany.

Patino, L. C., M. Carr, and M. D. Feigenson (1997), Cross-arc geochemical variations in volcanic fields in Honduras C. A.: Progressive changes in source with distance from the volcanic front, *Contrib. Mineral. Petrol.*, *129*, 341–351.

Patino, L. C., M. Carr, and M. D. Feigenson (2000), Local and regional variations in Central American arc lavas controlled by variations in subducted sediment input, *Contrib. Mineral. Petrol.*, *138*, 256–283.

Pérez, W. and A. Freundt (2006), The youngest highly explosive basaltic eruptions from Masaya Caldera (Nicaragua): Stratigraphy and hazard assessment, in *Volcanic Hazards in Central America*, edited by W. I. Rose et al., *Spec. Pap. Geol. Soc. Am.*, *412*, 189–207.

Ranero, C., and R. von Huene (2000), Subduction erosion along the Middle of America convergent margin, *Nature*, *404*, 748–752.

Ranero, C. R., J. Phipps Morgan, K. McIntosh, and C. Reichert (2003), Bending-related faulting and mantle serpentinization at the Middle America trench, *Nature*, *425*, 367–373.

Ranero, C. R., A. Villaseñor, J. Phipps Morgan, and W. Weinrebe (2005), Relationship between bend-faulting at trenches and intermediate-depth seismicity, *Geochem. Geophys. Geosyst.*, *6*, Q12002, doi:10.1029/2005GC000997.

Ranero, C. R., I. Grevemeyer, H. Sahling, U. Barckhausen, C. Hensen, K. Wallmann, W. Weinrebe, P. Vannucchi, R. von Huene, and K. McIntosh (2008), Hydrogeological system of erosional convergent margins and its influence on tectonics and interplate seismogenesis, *Geochem. Geophys. Geosyst.*, doi:10.1029/2007GC001679, in press.

Reston, T. and J. Bialas (2002), RV SONNE, Cruise Report SO162, INGGAS-Test, Chile and Peru, *GEOMAR Rep. 103*, 114 pp., IFM-GEOMAR, Kiel, Germany.

Rüpke, L. H., J. P. Morgan, M. Hort, and J. A. D. Connolly (2002), Are the regional variations in Central American arc lavas due to differing basaltic versus peridotitic slab sources of fluids?, *Geology*, *30*, 1035–1038.

Syracuse, E. M., and G. A. Abers (2006), Global compilation of variations in slab depth beneath arc volcanoes and implications, *Geochem. Geophys. Geosyst.*, *7*, Q05017, doi:10.1029/2005GC001045.

Talukder, A. R., J. Bialas, D. Klaeschen, D. Buerk, W. Brueckmann, T. Reston, and M. Breitzke (2007), High-resolution, deep tow, multichannel seismic and sidescan sonar survey of the submarine mounds and associated BSR off Nicaragua Pacific margin, *Mar. Geol.*, *241*(1–4), 33–43.

Tappin, D. R., P. Watts, G. M. McMurtry, Y. Lafoy, and T. Matsumoto (2001), The Sissano, Papua New Guinea tsunami of July 1998: Offshore evidence on the source mechanism, *Mar. Geol.*, *175*, 1–23.

Vannucchi, P., S. Galeotti, P. Clift, C. Ranero, and R. von Huene (2004), Longterm subduction erosion along the Guatemalan margin of the Middle America Trench, *Geology*, *32*, 617–620.

von Huene, R., C. R. Ranero, and W. Weinrebe (2000), Quaternary convergent margin tectonics of Costa Rica, segmentation of the Cocos plate, and Central American volcanism, *Tectonics*, *19*, 314–334.

von Huene, R., C. Ranero, and P. Vannucchi (2004a), Generic model of subduction erosion, *Geology*, *32*(10), 913–916.

von Huene, R., C. R. Ranero, and P. Watts (2004b), Tsunamigenic slope failure along the Middle America Trench in two tectonic settings, *Mar. Geol.*, *203*, 303–317.